Inorganica Chimica Acta, *174* (1990) 155–159

A Structural Investigation of Several Mixed Lanthanide Orthophosphates

D. F. MULLICA, E. L. SAPPENFIELD
Department of Chemistry, Baylor University, Waco, TX 76798 (U.S.A.)
and L. A. BOATNER
Solid State Division, Oak Ridge National Laboratory, Oak Ridge, TN 37831 (U.S.A.)

(Received November 27, 1989)

Abstract

The single crystal structures of $Gd_{0.5}Er_{0.5}PO_4$, $Gd_{0.5}Y_{0.5}PO_4$, $Gd_{0.5}Yb_{0.5}PO_4$ and $Gd_{0.75}Yb_{0.25}PO_4$ have been determined by means of single crystal X-ray diffraction techniques. These mixed phosphate compounds have the zircon-type structure and are therefore isostructural with the pure orthophosphates of the higher lanthanides (i.e. Tb, Dy, ..., Lu). The subject mixed orthophosphates crystallize in space group $I4_1/amd$ (D_{4h}^{19}, No. 141). Anisotropic refinement of the structures using a full-matrix least-squares program yielded final reliability factors in the range of 0.040 to 0.053. The metal atoms in each compound are eight coordinated to oxygen atoms, with two distinct M–O bond distances. The important bond distance $P–O_{av.}$ was found to be 1.533(6) Å. The coordination geometry about the central metal atom is bisphenoidal (D_{2d}) and is represented by two interpenetrating tetrahedra. In each mixed compound, the phosphate group is found to be a distorted tetrahedron.

Introduction

Materials for the long-term disposal of nuclear wastes must be both chemically and physically stable over geologic periods of time and they must be able to endure unusually hostile conditions, including high levels of radiation, high temperatures and chemically active ground waters. These restrictive conditions have lead to the investigation of the highly insoluble lanthanide and mixed orthophosphates as potential primary host for nuclear waste disposal [1–3].

Lanthanide orthophosphates exist in two different structural types. The first half of the lanthanide series (Ln = La, ..., Gd) crystallizes in the monoclinic monozite-type structure while the higher-atomic-number rare-earths (RE = Tb, ..., Lu, Sc, and Y) exist as the xenotine or zircon-type structure [4, 5]. Orthophosphates of yttrium, scandium and lutetium doped with gadolinium were extensively studied previously by Rappaz *et al.* using EPR spectroscopy [6]. These workers showed that a gadolinium impurity occupies exactly the same substitutional site as the heavy metal cation in the host orthophosphate material. The ability of EPR to verify that impurities at the level of up to 1 or 2 atm.% continue to occupy a given crystallographic site following a multi-step processing sequence, and that they do not become complexed with possible point defects or occupy interstitial sites in the host lattice, is important to assuring the solid state chemical properties of potential nuclear waste materials.

In contrast to the earlier work of Rappaz *et al.* the present investigation is concerned with the structural properties of mixed orthophosphates with relatively high concentrations of different heavy metal cations. EPR spectroscopy is not applicable to the investigation of a mixed system of this type with ‘impurities’ at such elevated concentrations, and techniques such as single crystal X-ray structural refinements must be utilized in order to obtain solid state chemical information that can be applied to the prediction of the properties and prolonged stability of mixed orthophosphates systems [2, 7].

Experimental

X-ray Crystal Analysis

Using the appropriated molar ratios of the subject rare-earth oxides, single crystals of $Gd_{0.50}Er_{0.50}PO_4$, $Gd_{0.50}Y_{0.50}PO_4$, $Gd_{0.50}Yb_{0.50}PO_4$ and $Gd_{0.75}Yb_{0.25}PO_4$ were synthesized by previously described methods [6, 7]. A single crystal of each compound was selected on optical quality and mounted on a glass fiber for single crystal X-ray diffraction analysis. The crystals were analyzed using an Enraf-Nonius CAD4 diffractometer equipped with a dense graphite monochromator (5.8° take-off angle). Unit cell parameters were determined using the Enraf-Nonius subroutines SEARCH, INDEX and LEAST SQUARES. A least-squares fit of 20 (1:1 Gd/Er), 19 (1:1 Gd/Y), 25 (1:1 Gd/Yb) and 25 (3:1 Gd/Yb) well centered reflections was used to determine unit cell parameters (see Table 1) and orientation matrices

0020-1693/90/$3.50

TABLE 1. Crystal data and statistical summaries

	Gd/ErPO$_4$^{a}	Gd/YPO$_4$^{a}	Gd/YbPO$_4$^{a}	Gd/YbPO$_4$^{b}
Space group	$I4_1/amd$	$I4_1/amd$	$I4_1/amd$	$I4_1/amd$
a (Å)	6.880(2)	6.914(3)	6.865(2)	6.903(2)
b (Å)	6.880(2)	6.914(3)	6.865(2)	6.903(2)
c (Å)	6.017(2)	6.042(4)	6.004(2)	6.034(2)
V (Å^3)	284.8	288.8	283.0	287.5
D_x (Mg m^{-3})	5.999	5.013	6.103	5.917
Z	4	4	4	4
M_r	257.23	218.05	260.12	256.17
$F(000)$ (e)	452	394	456	450
Crystal size (mm)	0.24 × 0.28 × 0.47	0.32 × 0.18 × 0.70	0.29 × 0.40 × 0.50	0.31 × 0.30 × 0.58
μ (Mo K$\bar{\alpha}$) (cm^{-1})	26.63	22.05	28.63	27.81
Transmission range				
min.	0.9374	0.9054	0.9547	0.9491
max.	0.9943	0.9926	0.9980	0.9995
$\Delta\theta$ (°)	1.5 - 45.0	1.5 - 45.0	1.5 - 45.0	1.5 - 45.0
R_{int}	0.030	0.035	0.051	0.045
R	0.043	0.041	0.053	0.049
R_w	0.041	0.040	0.050	0.048
g ($\times 10^{-6}$ e^{-2})	11.8	7.0	6.4	5.5
Reflections ($I > 3\sigma(I)$)	289	279	261	279
Goodness of fit (Σ_2)	2.32	1.71	2.78	2.39
Shift/error				
max. (10^{-5})	1.3	1.6	1.1	0.6
av. (10^{-6})	3.7	5.2	4.3	0.15

^{a}Compound with a 50:50 mixture. ^{b}Compound with a 75:25 mixture.

used for the data collection process. Intensity data were obtained by employing the ω–2θ scan technique at a rate of 0.38 to 3.35° min^{-1} which was determined by a fast prescan of 3.35° min^{-1}. The data were collected using Mo K$\bar{\alpha}$ radiation (λ_{mean} = 0.71073 Å) in the range of $3.0 < 2\theta < 90°$ at a variable scan width of 1.25 + 0.35 tanθ. In order to check the reliability and stability of the electronic hardware and crystals, two reflections were monitored for each compound every 2 h of exposure time. The deviations of the intensity data for the standard reflections were less than 0.5% for all compounds throughout the entire data collection. Reflections having less than 75 counts above background during the prescan were considered to be unobserved. Intensities having $I > 3\sigma(I)$ were used in the structure refinement. Experimental and statistical data are listed in Table 1 for the compounds studied.

Structural Refinement

Systematic absences revealed appropriate space group assignment to be $I4_1/amd$ for each of the compounds investigated. All of the data were corrected for Lorentz and polarization factors in addition to absorption effects. Absorption corrections were applied using crystal shape and dimensions to calculate the X-ray pathlength. The numerical absorption [8] correction is based on Gaussian integration techniques described by Coppens *et al.* [9]. The data were averaged (R_{int}) (see Table 1), and initial atomic positions for the metals, phosphorous and oxygen atoms were taken from the pure isostructural lanthanide orthophosphates [5]. Initial structural refinement was accomplished isotropically using a full-matrix least-squares program [8]. Anisotropic refinement of the thermal parameters and the application of secondary extinction corrections (g) yielded final reliability factors based on $R = \Sigma\Delta F/\Sigma F_o$ and $R_w = \Sigma\sqrt{w}\Delta F/\Sigma\sqrt{w}F_o$ where ΔF is defined as $||F_o| - |F_c||$. The weighting factor w is defined as the reciprocal of the square of the standard deviation on F_o, $\sigma^{-2}(F_o)$. The occupancies of the metal atoms were refined but did not deviate appreciably from the set values. These occupancy values were confirmed by semi-quantitative X-ray fluorescence analysis using a Novascan 30 scanning electron microscope equipped with a PGT microprobe. Table 1 lists the 'goodness-of-fit' values and the maximum abscission values $[\Delta\zeta_i/\zeta_i]$ where ζ_i are varied parameters. The final difference Fourier map revealed only random background fluctuations except in the vicinity of the lanthanide metal atoms where the electron density residual was minimal. Anomalous dispersion correction factors and scattering factors for each atom were obtained from the work of Ibers and Hamilton [10]. Final atomic positions, occupancies and equivalent

TABLE 2. Atomic positional parameters ($\times 10^3$) and equivalent isotropic thermal parameters ($\times 10^4$)

Atom	Occupancy	x	y	z	U_{eq} (Å^2)^a
Gd	0.50(1)	0	750	125	42(1)
Er	0.50(1)	0	250	875	29(1)
P	1.00	0	250	375	55(4)
O	1.00	0	424.7(8)	216.6(9)	67(8)
Gd	0.50(1)	0	750	125	91(1)
Y	0.50(1)	0	250	875	143(3)
P	1.00	0	250	375	84(3)
O	1.00	0	423.7(7)	217.6(8)	114(7)
Gd	0.50(1)	0	750	125	55(1)
Yb	0.50(1)	0	250	875	41(1)
P	1.00	0	250	375	81(5)
O	1.00	0	425(1)	214(1)	100(10)
Gd	0.75(1)	0	750	125	54(1)
Yb	0.25(1)	0	250	875	59(2)
P	1.00	0	250	375	65(4)
O	1.00	0	423(1)	218(1)	90(10)

[a] Isotropic equivalent thermal parameter (U_{eq}) defined as one-third the trace of the orthogonalized U_{ij} tensor.

isotropic thermal parameters with the estimated standard deviations are listed in Table 2. See also 'Supplementary Material'.

Discussion

The single crystal analyses of the compounds investigated here indicate that each substance crystallizes in the space group $I4_1/amd$ (No. 141) and has the zircon-type structure. A stereoview of the unit cell of the tetragonal orthophosphates is shown in Fig. 1. The arrangement of the oxygen atoms about the metal atoms is shown in Fig. 2, which is a representative of each of the investigated orthophosphates. The eight coordinated metal is apparent as well as the linkage provided by the distorted tetrahedral phosphate groups. Eight oxygen atoms are coordinated to the metal atom at two distinct M–O distances (see Table 3). Each unique distance forms a distorted tetrahedron, and the tetrahedra are oriented perpendicular to each other. This arrangement of the oxygen atoms has been described as a bisbisphenoidal polyhedron (dodecahedron) [11, 12]. M–O bond distances are well within the values compiled in BIDICS [13]. The phosphate group in each compound is a distorted tetrahedron as evidenced by the separate O–P–O bond angles presented in Table 3. The phosphorous–oxygen bond distances are in excellent agreement with the values found in the literature [13] as well as with the summation of the involved radii of phosphorous and oxygen ions found in the work of Shannon [14], i.e. 1.53 Å (see Table 3 for comparisons, the mean P–O distance is 1.533(6) Å). Each oxygen atom is coordinated to three atoms – one phosphorous and two metal atoms.

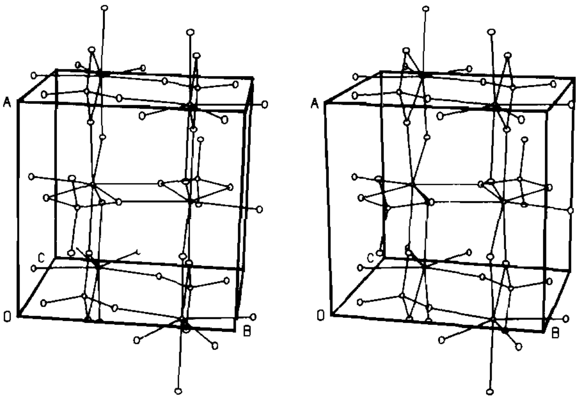

Fig. 1. A representative stereoscopic view of the molecular packing within the unit cell of the zircon-type structure. The orientation clearly shows the bridging effect between molecules.

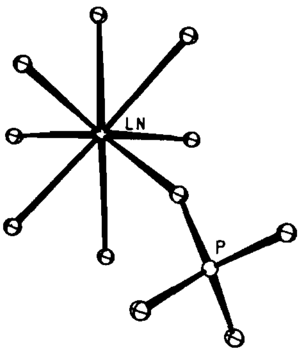

Fig. 2. Tetragonal Ln/LnPO$_4$. The interpenetrating tetrahedral sets (bisphenoidal arrangement) are readily seen as well as the tetrahedral orientation of the phosphate group.

TABLE 3. Bond and contact distances (Å) and angles (°)

	Gd/ErPO$_4$ [a]	Gd/YPO$_4$ [a]	Gd/YBPO$_4$ [a]	Gd/YbPO$_4$ [b]
M–O	2.305(4) 2.381(4)	2.324(4) 2.393(4)	2.294(5) 2.365(5)	2.327(5) 2.389(5)
Average	2.343	2.359	2.330	2.358
P–O	1.534(4)	1.532(4)	1.542(5)	1.524(5)
Phosphate group				
O(1)–O(2) O(3)–O(4)	2.403(7)	2.402(7)	2.404(10)	2.387(9)
O(1)–O(3), O(4) O(2)–O(3), O(4)	2.554(6)	2.550(6)	2.573(9)	2.538(8)
O(1)–P–O(2) O(3)–P–O(4)	103.2(3)	103.2(3)	102.5(4)	103.1(3)
O(1)–P–O(3), O(4) O(2)–P–O(3), O(4)	112.7(2)	112.7(1)	113.1(2)	112.8(2)
Average	109.5	109.5	109.6	109.6

[a] Compounds containing a 50:50 mixture. [b] Compound containing a 75:25 mixture.

The metal and phosphorous atoms occupy special sites in the unit cell. The metal atoms in these mixed systems are disordered and have occupancies according to each compound's molecular formula. In each case, the occupancies of the metal atom were refined based on the multiplicity of the special site. The refined values of the multiplicities did not vary appreciable from the theoretical value of one-half occupancy in the case of Gd/Er, Gd/Y and Gd/Yb, and three-quarters for the Gd in $Gd_{0.75}Yb_{0.25}PO_4$. These occupancy values were confirmed through X-ray fluorescence analysis.

The cell parameters for the mixed orthophosphates are within the range of values for pure metal–cation compounds with the zircon-type structure [15, 16]. The Gd/Er mixed system cell parameters correspond quite well with the cell parameters of pure holmium orthophosphate, while Gd/Y corresponds with dysprosium orthophosphate, and Gd/Yb (1:1) corresponds with erbium orthophosphate. For the Gd/Yb (3:1) compound, however, the cell parameters are between the cell parameters for pure dysprosium and holmium orthophosphate. This relationship of the cell parameters also parallels the relationship of the effective ionic radii. Previously, the dependence of the effective ionic radii on the cell parameters of the rare-earth orthophosphates has been established by Milligan *et al.* [16]. The experimentally determined effective ionic radii using the empirical relationship of Milligan *et al.* [16], however, are smaller than the values obtained by direct averaging of the ionic radii of each pair of metal atoms. This effect appears to be the result of the molecular packing in the crystal lattice. Due to the previously noted interest in the lanthanide orthophosphates as a primary host for high-level nuclear wastes, such molecular packing effects are significant and may have practical implications.

Supplementary Material

Structure factor tables and anisotropic thermal parameters are available from author D.F.M.

Acknowledgements

Research sponsored by Division of Material Sciences, U.S. Department of Energy under contract no. DE-AC05-84OR21400 with Martin Marietta Energy Systems, Inc. The authors acknowledge the financial support, in part, by the Robert A. Welch Foundation (Grant No. AA-668) and Baylor University.

References

1 G. J. McCarthy, W. B. White and D. E. Pfoertsch, *Mater. Res. Bull., 13* (1978) 1239.

2 L. A. Boatner, G. W. Beall, M. M. Abraham, C. B. Finch, P. G. Huray and M. Rappaz, in C. J. Northrup (ed.), *Scientific Basis for Nuclear Waste Management*, Vol. 2, Plenum, New York, 1980, p. 289.

3 M. Petek, M. M. Abraham and L. A. Boatner, in S. V. Topp (ed.), *Scientific Basis for Nuclear Waste Management*, Vol. 4, Elsevier-North Holland, The Netherlands, 1982, p. 181.

4 F. Weigel, V. Scherer and H. Henschel, *J. Am. Ceram. Soc., 48* (1965) 383.

5 W. O. Milligan, D. F. Mullica, G. W. Beall and L. A. Boatner, *Inorg. Chim. Act, 70* (1983) 133.

6 L. A. Boatner, G. W. Beall, M. M. Abraham, C. B. Finch, R. J. Floran, P. G. Huray and M. Rappaz, *Management of Alpha-Contaminated Wastes, IAEA-SM-245/73,* International Atomic Energy Agency, Vienna, 1981, p. 411.

7 M. Rappaz, L. A. Boatner and M. M. Abraham, *J. Chem. Phys., 73* (1980) 1095.

8 Enraf-Nonius, *Enraf-Nonius VAX Structural Determination Package,* Delft, The Netherlands, 1982.

9 P. Coppens, L. Leserowitz and D. Rabinovich, *Acta Crystallogr., 18* (1965) 1035.

10 J. A. Ibers and W. C. Hamilton, *International Tables for X-ray Crystallography,* Vol. IV, 1974, p. 72.

11 D. F. Mullica, D. A. Grossie and L. A. Boatner, *Inorg. Chim. Acta, 118* (1986) 173.

12 F. A. Cotton and G. Wilkenson, *Advanced Inorganic Chemistry,* Wiley, New York, 1980, pp. 53 - 54.

13 *Bond Index of the Determination of Inorganic Crystal Structures,* BIDICS, Institute for Material Research, Hamilton, Canada, 1969–1981.

14 R. D. Shannon, *Acta Crystallogr., Sect. A., 32* (1976) 751.

15 W. O. Milligan, D. F. Mullica, G. W. Beall and L. A. Boatner, *Acta Crystallogr., Sect. C, 39* (1983) 23.

16 W. O. Milligan, D. F. Mullica, H. O. Perkins, G. W. Beall and L. A. Boatner, *Inorg. Chim. Acta, 77* (1983) L23.